

This is an Open Access document downloaded from ORCA, Cardiff University's institutional repository: <https://orca.cardiff.ac.uk/id/eprint/111524/>

This is the author's version of a work that was submitted to / accepted for publication.

Citation for final published version:

Kaouri, Katerina , Allwright, D.J., Chapman, C.J. and Ockendon, J.R. 2008. Singularities of wavefields and sonic boom. *Wave Motion* 45 (3) , pp. 217-237. 10.1016/j.wavemoti.2007.06.003

Publishers page: <http://dx.doi.org/10.1016/j.wavemoti.2007.06.003>

Please note:

Changes made as a result of publishing processes such as copy-editing, formatting and page numbers may not be reflected in this version. For the definitive version of this publication, please refer to the published source. You are advised to consult the publisher's version if you wish to cite this paper.

This version is being made available in accordance with publisher policies. See <http://orca.cf.ac.uk/policies.html> for usage policies. Copyright and moral rights for publications made available in ORCA are retained by the copyright holders.



# Singularities of Wavefields and Sonic Boom

K. Kaouri<sup>a,1</sup>, D.J. Allwright<sup>b</sup>, C.J. Chapman<sup>c</sup>, J.R. Ockendon<sup>b</sup>

<sup>a</sup>*Centre for Mathematical Medicine and Biology, School of Mathematical Sciences,  
The University of Nottingham, University Park, Nottingham, NG7 2RD, UK  
katerina.kaouri@maths.nottingham.ac.uk.*

<sup>b</sup>*Oxford Centre for Industrial and Applied Mathematics (OCIAM), Mathematical  
Institute, 24-29 St Giles', Oxford OX1 3LB, UK*

<sup>c</sup>*Department of Mathematics, University of Keele, Keele, Staffordshire, ST5 5BG,  
UK*

---

## Abstract

This paper analyses the generic singularities that can occur in wavefields driven by point acoustic sources moving steadily or accelerating in homogeneous or stratified atmospheres. These situations are unified by the result that the strongest wavefields satisfy the Tricomi equation, except in cases of very strong focusing of acoustic rays. The implications for sonic boom carpets are discussed.

*Key words:* linear wave theory, accelerating source, stratified medium, sonic boom, Tricomi equation, boom ray, Mach envelope

*PACS:*

---

## 1 Introduction

This paper concerns the mathematical description of some of the common singularities that can occur in the acoustic wavefields emitted by a localised sound source moving in a homogeneous or inhomogeneous atmosphere. Most of our investigations have been stimulated by the need to gain better understanding of secondary and primary sonic boom, and models for these two phenomena will form the basis of our discussion. The former concerns the singularities produced in the acoustic field generated

---

<sup>1</sup> Part of this work is contained in the DPhil (PhD) thesis of K. Kaouri, and it was undertaken at the University of Oxford [8].

by a supersonic source moving horizontally in an atmosphere in which the ambient sound speed,  $c$ , varies; we will pay particular attention to atmospheres where the sound speed increases with distance above the source and attains the source speed at a critical height. The latter concerns the analogous singularities in the sound field of a point source accelerating in a homogeneous atmosphere, with its speed varying through the ambient sound speed. The mathematical descriptions appropriate to each will be seen to be closely related to each other.

Our principal aim is to find representations for the singularities of the solution of the wave equation

$$\frac{\partial^2 \phi}{\partial x^2} + \frac{\partial^2 \phi}{\partial y^2} + \frac{\partial^2 \phi}{\partial z^2} = \frac{1}{c^2} \frac{\partial^2 \phi}{\partial t^2} \quad (1)$$

that are both relevant to sonic boom and simple enough for us to be able to give a precise local description of the wavefield. In the remainder of the introduction, we will review the background geometry and analysis associated with the singularities and then in §2-§5 we will find their precise form.

The usual analysis of singularities of the solution of (1) starts from representing the solution as a superposition of pulses emitted from the source [1]. Indeed, when  $c$  is constant this can be done explicitly, using the retarded potential solution. But in any case, each pulse engenders a *wavefront* that propagates in space, and the normals to these wavefronts form a three-parameter family of *rays* in  $(x, y, z)$  coordinates.<sup>2</sup> Moreover, in the cases in which we are interested, the wavefronts will have a *wave envelope* or *Mach envelope* which is a time-dependent surface in  $(x, y, z)$ -space and we will call the special rays that terminate on the Mach envelope the *boom rays*. At any instant of time, there will be a two-parameter family of boom rays embedded in the three-parameter family of “ordinary” rays.<sup>3</sup>

In this paper, the Mach envelope will be central to our discussion because

---

<sup>2</sup> In mathematical terms, it is usual to think of rays as being the generators (or **bicharacteristics**) of the **ray cone** (or **characteristic cone**) emanating from the point source when it is at any particular point in the  $(x, y, z, t)$ -space. The physical wavefronts at time  $t = t_0$  are the intersections of all the ray cones with the plane  $t = t_0$  and the physical rays are the projections of the bicharacteristics onto this plane.

<sup>3</sup> As the source moves, the ray cones will usually envelop a characteristic surface generated by boom “bicharacteristics” whose intersection with  $t = t_0$  is the Mach envelope.

it is only on this envelope that  $\phi$  can have singularities. As we shall see, many kinds of such singularities are possible, especially when the Mach envelope itself has singularities. The simplest situation is for an instantaneous  $\delta$ -function source at the origin, whose wavefield is the fundamental solution of (1). When  $c$  is constant and we are in two or three dimensions the wavefield is respectively  $H(ct - r)/\sqrt{c^2t^2 - r^2}$  and  $\delta(r - ct)/r$ , where  $r$  denotes the radial coordinate and  $H$  is the Heaviside function. The only singularities are at the wavefront  $r = ct$  and the rays are radial. However, when the source is moving a Mach envelope can be formed and the singularities which it supports are less easy to discern. For example, for a point source accelerated impulsively to constant supersonic speed, along the negative  $x$ -axis, we expect the wavefront picture to be as in Figure 1, with the Mach envelope being the well-known Mach wedge or cone. The normals to the Mach envelope, starting at the source and terminating at the envelope, are the boom rays.

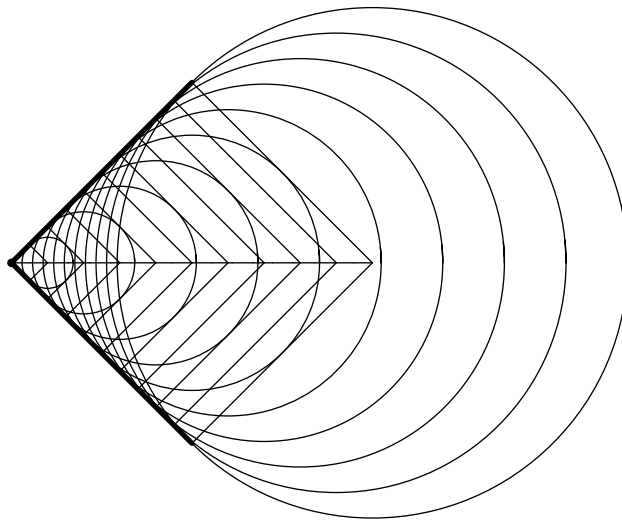


Fig. 1. Wavefronts (circles), boom rays and the Mach envelope (bold) for a source accelerated impulsively to constant supersonic speed, from right to left.

For a smoothly accelerated source Figure 1 is replaced by Figure 2, in which the Mach envelope has two components joined at a cusp at any instant after that at which the source passed the sound speed (Lilley et al. [7]). In §3, we will show that the singularity at the cusp is stronger than at either Mach envelope component and, as time evolves, the cusps form a locus which, in the cases of two-dimensional or axisymmetric flow, is the envelope of the boom rays terminating at one of the two components of the Mach envelope, as shown in Figure 3.

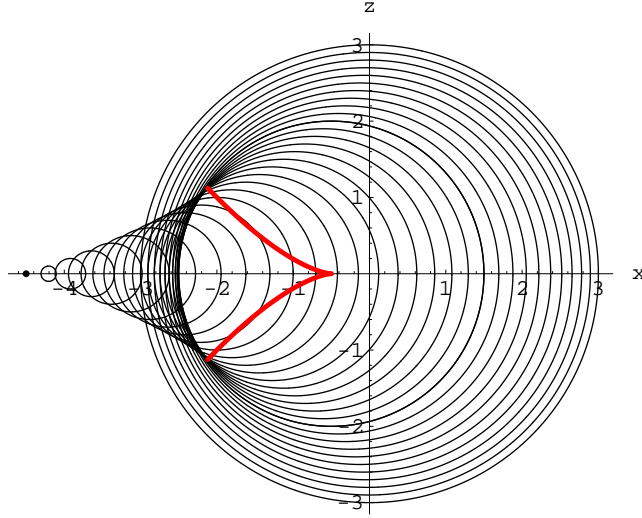


Fig. 2. The wavefronts for a source smoothly accelerated through the sound speed, from right to left. The Mach envelope has “front” and “back” components joined by cusps. The thicker line is the cusp locus.

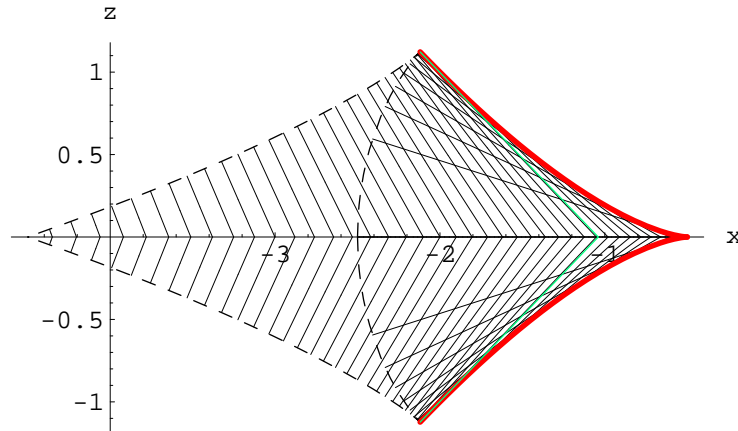


Fig. 3. Boom rays for a source smoothly accelerating through the sound speed. The Mach envelope, which consists of two components joined by cusps, is the dashed line. One family of boom rays terminates at one component of the Mach envelope and the other family of boom rays terminates at the other component. The second family of boom rays forms an envelope (shown with a thicker line), which is also the locus of the cusps.

Figures 4 and 5 show the corresponding figures for the travelling wave solution for steady wave propagation in a stratified atmosphere, resulting from a supersonic source moving horizontally below a “sonic height” at which the sound speed equals the source speed. The locus of the cusps joining the two Mach envelope components is the sonic height, which is again an envelope of boom rays. The cusps in the Mach envelope of Figures 2, 4 both move with the local sound speed. Although the locus of *wavefront* cusps in Figure 4 (dashed line) could technically be thought of as a wave envelope in  $(x, z)$ -space it is not the projection in this space

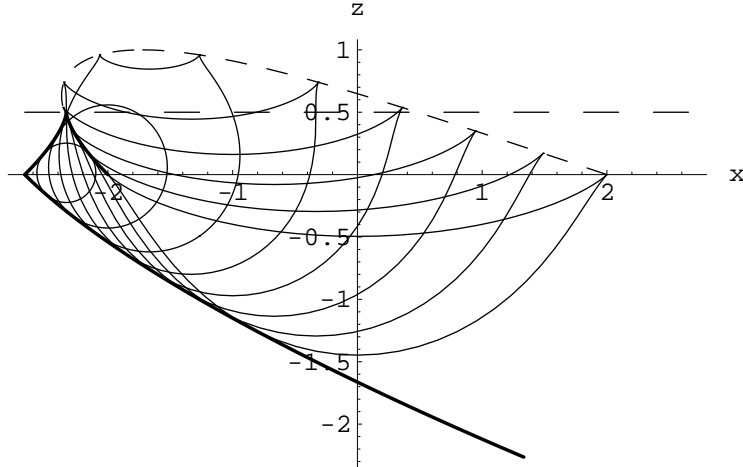


Fig. 4. The wavefronts in  $z < 1$  and the Mach envelope for a source moving with speed  $U = \sqrt{2}$  in the atmosphere  $c = 1/\sqrt{1-z}$ . The “sonic height”  $z = 1/2$  is the locus of the Mach envelope cusps. (The dashed curve is the locus of the wavefront cusps.) We have ignored waves radiated downwards from  $z = 1$ .

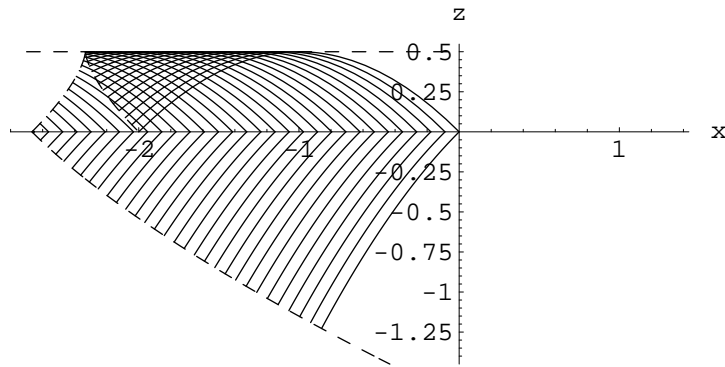


Fig. 5. Boom rays for a source moving with speed  $U = \sqrt{2}$  in the atmosphere  $c = 1/\sqrt{1-z}$ . The family of boomrays that terminate at the reflected component of the Mach envelope themselves form an envelope. The Mach envelope is the dashed line.

of a Mach envelope in  $(x, z, t)$ -space, and there will be no singularities of the wavefield on this locus. Neither are there any singularities at the cusp locus in Figure 2, except at the cusp itself.<sup>4</sup>

Before investigating these types of singularity in detail, we can anticipate the structure of the singularity near a Mach envelope cusp by considering wavefields that have rapid variations near a point moving along the cusp locus with the local sound speed, as mentioned above. Suppose, for example, that the problem is two-dimensional, with  $\phi = \phi(x, z, t)$ , and that the cusp locus,  $C$  say, is  $(x_0(t), z_0(t))$ , so that the local sound speed

<sup>4</sup> It is common in the aeronautical literature to focus attention on the cusps in the Mach envelope and this can be done without reference to the wavefronts by simply finding the boomrays and plotting their envelope; the cusp is located at the extremity of the envelope.

is  $c_0(t) = c(x_0(t), z_0(t))$ . We make the key assumption that the curvature of  $C$  differs from the curvature of the family of boom rays forming it.<sup>5</sup> We write

$$\dot{x}_0(t) = c_0(t) \cos \theta(t), \quad \dot{z}_0(t) = c_0(t) \sin \theta(t), \quad (2)$$

so that  $\theta(t)$  is the local slope of  $C$ . Then near the point of interest we want to change to local coordinates  $(\xi, \zeta)$  along and normal to  $C$ , so that

$$\begin{pmatrix} \xi \\ \zeta \end{pmatrix} = \begin{pmatrix} \cos \theta & \sin \theta \\ -\sin \theta & \cos \theta \end{pmatrix} \begin{pmatrix} x - x_0 \\ z - z_0 \end{pmatrix}. \quad (3)$$

We must transform (1) from  $(x, z, t)$  to  $(\xi, \zeta, t)$ , using

$$\left( \frac{\partial}{\partial x} \right)_{z,t} = \cos \theta \left( \frac{\partial}{\partial \xi} \right)_{\zeta,t} - \sin \theta \left( \frac{\partial}{\partial \zeta} \right)_{\xi,t}, \quad (4)$$

$$\left( \frac{\partial}{\partial z} \right)_{x,t} = \sin \theta \left( \frac{\partial}{\partial \xi} \right)_{\zeta,t} + \cos \theta \left( \frac{\partial}{\partial \zeta} \right)_{\xi,t}, \quad (5)$$

$$\left( \frac{\partial}{\partial t} \right)_{x,z} = (-c_0 + \zeta \dot{\theta}) \left( \frac{\partial}{\partial \xi} \right)_{\zeta,t} - \xi \dot{\theta} \left( \frac{\partial}{\partial \zeta} \right)_{\xi,t} + \left( \frac{\partial}{\partial t} \right)_{\xi,\zeta}. \quad (6)$$

The equation in full is then

$$\begin{aligned} & \phi_{tt} - \dot{c}_0 \phi_\xi - 2c_0 \phi_{\xi t} + \zeta \ddot{\theta} \phi_\xi + 2\zeta \dot{\theta} \phi_{\xi t} - \xi \ddot{\theta} \phi_\zeta - 2\xi \dot{\theta} \phi_{\zeta t} + c_0^2 \phi_{\xi\xi} - 2c_0 \zeta \dot{\theta} \phi_{\xi\xi} \\ & \quad + c_0 \dot{\theta} \phi_\zeta + 2c_0 \xi \dot{\theta} \phi_{\xi\zeta} + \zeta^2 \dot{\theta}^2 \phi_{\xi\xi} - \zeta \dot{\theta}^2 \phi_\zeta - 2\xi \zeta \dot{\theta}^2 \phi_{\xi\zeta} - \xi \dot{\theta}^2 \phi_\xi + \xi^2 \dot{\theta}^2 \phi_{\zeta\zeta} \\ & = c^2 (\phi_{\xi\xi} + \phi_{\zeta\zeta}) \\ & = (\phi_{\xi\xi} + \phi_{\zeta\zeta}) \left( c_0^2 + 2c_0 \left. \frac{\partial c}{\partial x} \right|_0 (\xi \cos \theta - \zeta \sin \theta) + \right. \\ & \quad \left. 2c_0 \left. \frac{\partial c}{\partial z} \right|_0 (\xi \sin \theta + \zeta \cos \theta) + O(\xi^2 + \zeta^2) \right). \end{aligned} \quad (7)$$

On the right we have expanded  $c(x, z)^2$  as a Taylor series since we are interested in the local behaviour near  $(x_0, z_0)$ . In this equation, the term  $c_0^2 \phi_{\xi\xi}$  cancels, and the distinguished limit we wish to consider is when  $\xi = \epsilon^{3/2} \Xi$  and  $\zeta = \epsilon Z$ , so that we write

$$\phi = \phi(\Xi, Z, t) = \phi(\epsilon^{-3/2} \xi, \epsilon^{-1} \zeta, t). \quad (8)$$

<sup>5</sup> For example, in Figure 3 the cusp locus is curved and the boom rays are straight whereas in Figure 5 the cusp locus is straight but the boom rays are curved.

In this limit, the leading terms, at order  $\epsilon^{-2}$ , are

$$-2c_0 Z \dot{\theta} \phi_{\Xi\Xi} = c_0^2 \phi_{ZZ} + 2c_0 Z \phi_{\Xi\Xi} \left( \frac{\partial c}{\partial z} \Big|_0 \cos \theta - \frac{\partial c}{\partial x} \Big|_0 \sin \theta \right). \quad (9)$$

The quantity in brackets is the derivative of  $c$  normal to the curve  $C$ , and we denote it by  $\partial c / \partial \zeta|_0$ . The equation is then

$$\frac{\partial^2 \phi}{\partial Z^2} + \frac{2}{c_0} \left( \dot{\theta} + \frac{\partial c}{\partial \zeta} \Big|_0 \right) Z \frac{\partial^2 \phi}{\partial \Xi^2} = 0, \quad (10)$$

which is Tricomi's equation, with the coefficient depending on the difference in curvature between the curve  $C$  and the local curvature of the boom rays whose envelope it is. If, for example,  $C$  lies to the right of the boom rays, as seen by someone moving along the ray, then  $\dot{\theta} < -\partial c / \partial \zeta|_0$ , and the boom rays occupy the region  $Z > 0$ , which is the region to the left of  $C$  in Figures 3, 5. In either case the half-space occupied by the boom rays coincides with the half-space in which (10) is hyperbolic.

In §2 we will apply these ideas to the case of a point source that moves impulsively in a horizontally stratified atmosphere in two dimensions, as in Figures 4 and 5. Our analysis in terms of wavefronts will reveal the evolution of the Mach envelope reflection at the cusp and also indicate the three-dimensional generalisation.

In §3, we will consider a point source accelerating smoothly through the sound speed in a homogeneous atmosphere in two dimensions as shown in Figures 2 and 3. In this case we will have the luxury of the exact retarded potential solution against which we can check the predictions of (10).

Then, in §4 we will again use the retarded potential to describe a dramatic singularity proposed by Dempsey [2]. This can occur when the source accelerates more and more rapidly to hypersonic velocities, in which case the Mach envelopes can take the form of shrinking concentric circles. This generates a particularly violent singularity at a single point at just one instant of time.

Next, in §5 we will generalise these ideas to three dimensions in more detail, which will enable us to make two brief remarks about sonic boom "carpets". Finally, in the Appendix we will make some comments about the combined effects of acceleration and inhomogeneity.

## 2 Waves in a two-dimensional stratified atmosphere

We begin by considering wave propagation in two dimensions in an atmosphere in which there is a sonic height, so that, over some altitudes, the speed of sound increases with height. For the subsequent analysis, the simplest case is when  $c^2 = 1/(1 - z)$  in (1), where the source speed  $U$  is a constant, and we only consider the wavefield in the region  $z < 1$ , thereby ignoring all waves that may be reflected from, or generated in  $z \geq 1$ . We consider the canonical situation in which a unit point source moves impulsively along the  $x$ -axis. If this source is a monopole, (1) becomes

$$-\frac{\partial^2 \phi}{\partial x^2} - \frac{\partial^2 \phi}{\partial z^2} + (1 - z) \frac{\partial^2 \phi}{\partial t^2} = \delta(x + Ut) \delta(z) H(t). \quad (11)$$

Once this problem has been solved, the response to dipoles, etc., can be found by differentiation. For this choice of  $c(z)$  the wavefronts, boom rays and Mach envelope can all be calculated analytically.

The advantage of our choice of  $c$  is that if we move in the aerodynamic frame and seek a travelling wave solution of (11) in which  $\phi = \phi(\xi, z)$ ,  $\xi = x + Ut$ , we obtain

$$-\frac{\partial^2 \phi}{\partial z^2} - (1 - U^2 + U^2 z) \frac{\partial^2 \phi}{\partial \xi^2} = \delta(\xi) \delta(z), \quad (12)$$

which makes it easy to relate to (10). Our first step is to draw the wavefronts that are generated by the source. These are shown in the ‘‘subsonic’’ case  $U = \frac{1}{2}$  in Figure 6 and in the supersonic case  $U = \sqrt{2}$  in Figure 4. There is only a Mach envelope in the supersonic case and its most interesting part is formed by the tips of the upward-launched boomrays. These tips form two components of the envelope, namely an upward propagating component from the source and the reflection of this component from the sonic line  $z = \frac{1}{2}$ . These components have a very important qualitative difference; the former is outside the wavefronts, whereas the latter is inside the wavefronts. This difference is shown more clearly in the schematic Figure 7.

The boomrays of Figure 5 form a smooth envelope at the sonic line  $z = 1/2$ . The upward propagating component is formed by boomrays that have *not* touched this envelope but the reflected component is formed by

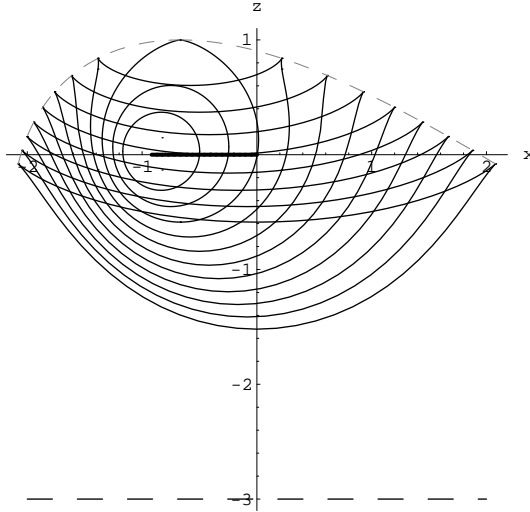


Fig. 6. Picture of the wavefronts for the subsonic motion with  $U = 1/2$  in the medium for which  $c = 1/\sqrt{1-z}$ . The sonic line ( $z = -3$ ) and the locus of wavefront cusps are shown with dashed lines.

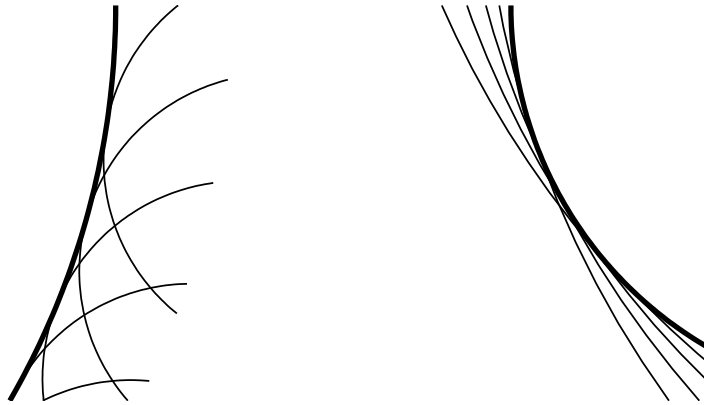


Fig. 7. Schematic diagrams that show the difference in the formation of the two components of the Mach envelope. In each case the thin curves are the wavefronts and the thick curve is their envelope. In the left picture the wavefronts are “inside” the envelope and in the right picture the wavefronts are “outside” the envelope.

boomrays that *have* touched the envelope. This is a second criterion for distinguishing between the two Mach envelope components.

With the translation  $z - \frac{1}{2} = Z$  and  $U = \sqrt{2}$  equation (12) becomes

$$\frac{\partial^2 \phi}{\partial Z^2} + 2Z \frac{\partial^2 \phi}{\partial \xi^2} = 0, \quad (13)$$

which is (10) with  $\Xi = \xi$  since  $c_0 = \sqrt{2}$ ,  $(\partial c / \partial \zeta)|_0 = \sqrt{2}$  and  $\dot{\theta} = 0$ . To obtain the boundary conditions that need to be imposed on (13) in order to reveal the structure of the singularity at the cusp of the Mach envelope, we begin by noting that, near the source,  $\phi$  is the Riemann function for

a wave equation with constant coefficients. Hence, the singularity on the Mach envelope is a jump in  $\phi$  from its value ahead of the envelope. There will be a nontrivial wavefield ahead of the envelope because of the waves emitted from the subsonic region  $Z > 1/2$ , but, as stated earlier, we will not consider this small wavefield here.

To understand how the jump in  $\phi$  propagates, we need to consider local solutions of (13) in the form  $\phi \sim Af\left(\left(\xi/\sqrt{2} - \frac{2}{3}(-Z)^{3/2}\right)/\varepsilon\right)$  for small  $\varepsilon$ , where  $A$  is an amplitude that is independent of  $\varepsilon$  to lowest order. Substituting into (13) and equating terms of  $O(\varepsilon^{-1})$  gives

$$\frac{\partial A}{\partial Z} - (-2Z)^{1/2} \frac{\partial A}{\partial \xi} + \frac{1}{4Z} A = 0. \quad (14)$$

Hence the variation of  $A$  along  $\frac{\xi}{\sqrt{2}} = \frac{2}{3}(-Z)^{3/2}$  is governed by

$$dA = \frac{\partial A}{\partial \xi} d\xi + \frac{\partial A}{\partial Z} dZ = -\frac{A}{4Z} dZ, \quad (15)$$

and thus  $A$  grows to be  $O(|Z|^{-1/4})$  as  $Z \rightarrow 0$ . Hence the far field boundary conditions for (13) are that

$$\phi \rightarrow 0 \text{ as } Z \rightarrow +\infty, \quad (16)$$

and

$$\phi \rightarrow |Z|^{-1/4} H\left(\frac{\xi}{\sqrt{2}} - \frac{2}{3}(-Z)^{3/2}\right) + \text{outgoing wave, as } Z \rightarrow -\infty. \quad (17)$$

The wavefield near the cusp can now be written down in terms of the transform  $\bar{\phi}(k, Z) = \int_{-\infty}^{\infty} \phi(\xi, Z) e^{ik\xi} d\xi$ . Since  $d^2\bar{\phi}/dZ^2 - 2k^2 Z \bar{\phi} = 0$ , we find that, as  $Z \rightarrow -\infty$ ,

$$\bar{\phi} \sim (-Z)^{-1/4} \left( \exp\left(\frac{ik(-2Z)^{3/2}}{3}\right) \bar{H}_+(k) + \exp\left(\frac{ik(-2Z)^{3/2}}{3}\right) \bar{H}_-(k) \right), \quad (18)$$

where  $\bar{H}_+(k)$  is the Fourier transform of the Heaviside function and  $\bar{H}_-(k)$  is to be determined. However, since we require that  $\phi$  should not grow exponentially as  $Z \rightarrow +\infty$ ,  $\bar{\phi}$  must be proportional to  $\text{Ai}(2^{1/3}k^{2/3}Z)$  and hence, from the connection formulae for the Airy function

$$\bar{H}_-(k) = \text{sgn}(k) \bar{H}_+(k) \quad (19)$$

and  $H_-$  is the Hilbert transform of  $H_+$ . This argument, which holds for any incoming wave and not just the Heaviside function in (17), reveals that the reflected Mach envelope is associated with a logarithmic singularity as  $Z \rightarrow -\infty$  with  $\xi/\sqrt{2} = -\frac{2}{3}(-Z)^{3/2}$ . This problem has, in various guises, been discussed by many authors over the years (Howarth [3], Lighthill [6], Guiraud [5], Rosales and Tabak [9], etc.). The representation of  $\phi$  as the Fourier transform of an Airy function is not convenient for describing its behaviour in more detail, except to confirm that  $\phi$  has no upstream influence in  $Z < 0$  for  $\xi/\sqrt{2} < \frac{2}{3}(-Z)^{3/2}$ . We can avoid connection formulae altogether if we write the general solution of (13) as

$$\phi(\xi, Z) = \int_{-\infty}^{\infty} F\left(\frac{\lambda^3}{3} + \lambda Z + \frac{\xi}{\sqrt{2}}\right) d\lambda, \quad (20)$$

for some function  $F$  for which the integral exists. Then (18) corresponds to setting

$$F(s) = H(s)/\sqrt{s}, \quad (21)$$

which leads us to an elementary integrand which can be analysed using the method of §3, and for which the singularities of  $\phi$  occur where  $9\xi^2 + 8Z^3 = 0$ .

### 3 Waves from an accelerating source in a homogeneous atmosphere

We begin by considering the singularities in the wavefield produced by a source accelerating along the negative  $x$ -axis in a homogeneous atmosphere. Generally, if the source position at  $t$  is  $x = X(t)$ , (11) is replaced by

$$-\frac{\partial^2 \phi}{\partial x^2} - \frac{\partial^2 \phi}{\partial z^2} + \frac{\partial^2 \phi}{\partial t^2} = \delta(x - X(t))\delta(z)H(t), \quad (22)$$

for which we have the explicit retarded potential solution

$$\phi = \frac{1}{2\pi} \int_0^t \frac{H(Q(\tau))d\tau}{\sqrt{Q(\tau)}}, \quad (23)$$

where  $Q(\tau) = (t - \tau)^2 - (x - X(\tau))^2 - z^2$ .

### 3.1 Impulsive Supersonic Motion

When  $X(t) = -Ut$ , with  $U = \text{constant}$  and  $U > 1$ , the wavefront geometry is as in Figure 1, and the Mach wedge is the Mach envelope. The wavefield is displayed graphically in Figure 8; it is simply the Riemann

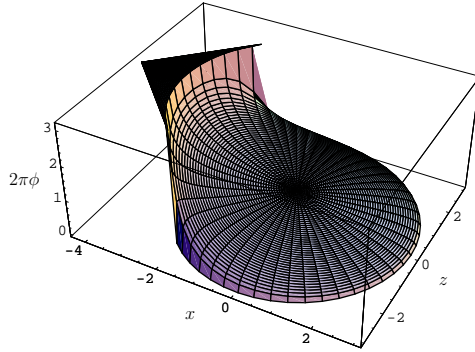


Fig. 8. Plot of the wavefield for a point source travelling with constant speed  $U = \sqrt{2}$  from right to left ( $c_0 = 1$ ).

function for the wave equation in the aerodynamic frame in the region between the Mach wedge and the circular wavefront  $x^2 + z^2 = t^2$ . Huygens' principle asserts that  $\nabla\phi$  should be zero in the aerodynamic frame inside the Mach wedge and we see that the wavefield conforms to this principle as soon as we are outside the wavefront  $x^2 + z^2 = t^2$ . Analytically, this happens because the limits of the integral in (23) become the two zeros of  $Q$  when we cross the wedge from the outside, and hence the integral becomes independent of  $x, z$  and  $t$ . Inside the wavefront  $x^2 + z^2 = t^2$ , the wavefield is given by

$$\phi = \frac{1}{2\pi\sqrt{U^2 - 1}} \arccos \left( \frac{xU + t}{\sqrt{(x + Ut)^2 - (U^2 - 1)z^2}} \right), \quad (24)$$

which joins continuously to the Riemann function in the Mach wedge (see Strang [10], [11], [12]).

### 3.2 Accelerating Source

The situation is more complicated when  $X(t) = -\frac{1}{2}t^2$ , so that the source traverses the sound speed when  $t = 1$ . The Mach envelope is

$$x(\tau; t) = -\frac{1}{2}\tau^2 - \frac{t - \tau}{\tau}, \quad z(\tau; t) = \pm(t - \tau) \left(1 - \frac{1}{\tau^2}\right)^{1/2}, \quad (25)$$

displayed in Figure 3. The cusps are where

$$\tau = \tau_c = t^{1/3}, \quad x = x_c = 1 - \frac{3}{2}t^{2/3}, \quad z = z_c = \pm(t^{2/3} - 1)^{3/2}. \quad (26)$$

There are, as we have seen in Figure 2, front and back components to the envelope. Figure 3 shows, with a thicker line, the cusp locus which is the envelope of the family of boom rays that terminate at the back component. As in §2, for a fixed time  $t$ , the boom rays that terminate at the front Mach envelope have not passed through the cusp locus, but the boom rays that terminate on the back Mach envelope have touched it.

Despite this apparent complexity, we have the convenient representation (23) for the wavefield everywhere, which we now analyse. On the Mach envelope,  $\phi$  again has a jump discontinuity because a local maximum of  $Q(\tau)$  passes downwards through zero as the Mach envelope is crossed. This is shown schematically as the transition  $C \rightarrow B \rightarrow A$  in Figure 9, and it is qualitatively similar to the supersonic motion of §3.1.

A local analysis can now be carried out by expanding  $Q(\tau)$  in the vicinity of a point  $\tau = \tau_E$  at which  $x = x_E$ ,  $z = z_E$  and  $t = t_E$  satisfy (25). Since the envelope is never parallel to the  $z$ -axis, we hold  $z_E$  fixed and since  $Q = \partial Q/\partial\tau = 0$  on the envelope, (25) means we can write

$$Q \approx \frac{2(t - \tau_E)}{\tau_E}(x - x_E) + \frac{t - \tau_E^3}{2\tau_E}(\tau - \tau_E)^2 + \dots \quad (27)$$

$Q$  is thus approximated by a quadratic in  $\tau$  whose roots are  $\tau_1, \tau_2$  say and in case  $A$  of Figure 9 the contribution from near  $\tau_E$  is zero. However, in case  $C$ , when  $t > \tau_E$ , this contribution is approximately

$$\frac{1}{2\pi} \sqrt{\frac{\tau_E}{\tau_E^3 - t}} \int_{\tau_1}^{\tau_2} \frac{d\tau}{\sqrt{(\tau_2 - \tau)(\tau - \tau_1)}} = \frac{1}{2} \sqrt{\frac{\tau_E}{\tau_E^3 - t}}. \quad (28)$$

On the back envelope, where  $1 \leq \tau < t^{1/3}$ , a similar analysis of the transition  $E \rightarrow F \rightarrow G$  in Figure 9 shows that the singular part of  $\phi$  is

$$-\frac{1}{2\pi} \sqrt{\frac{\tau_E}{t - \tau_E^3}} \ln |x - x_E|. \quad (29)$$

The contrast with (28) results from the fact that there are two contributions to  $\phi$  in  $E$  and only one in  $G$ . This necessitates integrating over  $\tau < \tau_E - \epsilon$  and  $\tau > \tau_E + \epsilon$  respectively where, from (27),  $\epsilon = \sqrt{2 \left( \frac{t - \tau_E}{t - \tau_E^3} \right)} (x_E - x)$ . It is this principal value calculation that spawns the logarithm in (29).

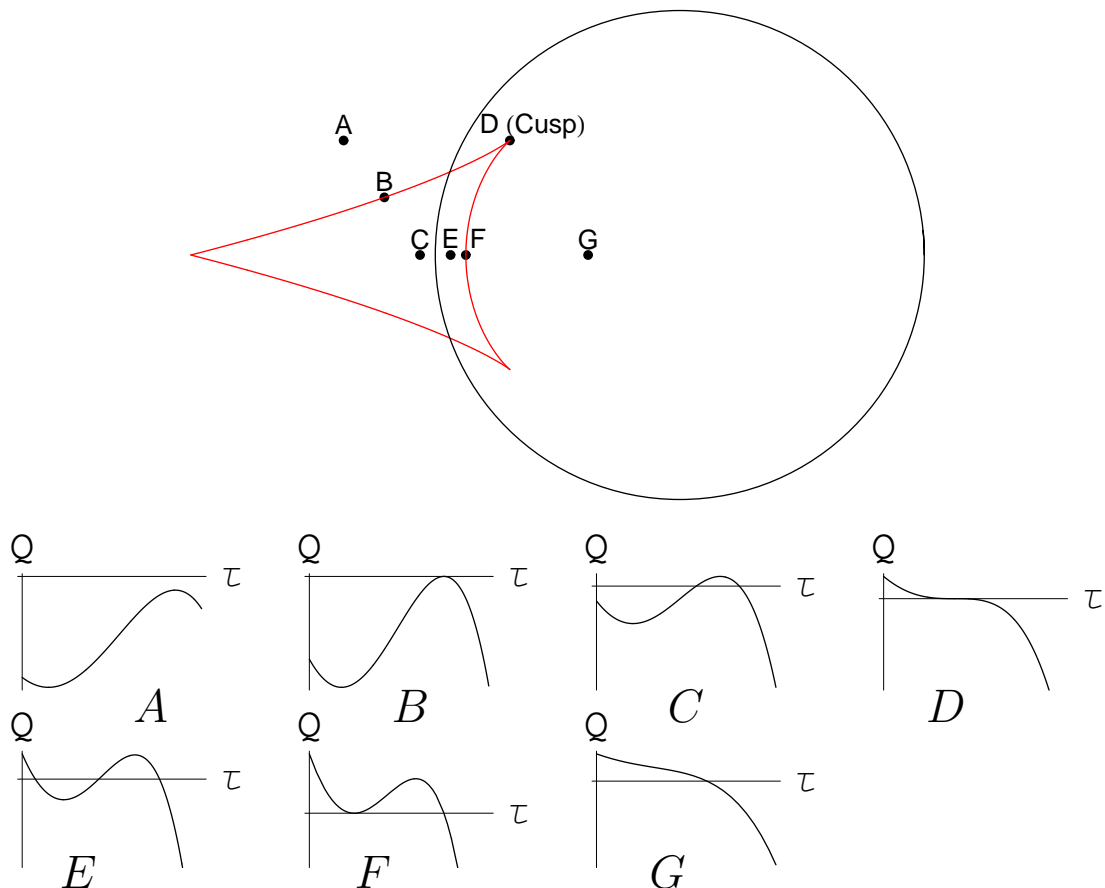


Fig. 9. The Mach envelope and the initial wavefront for a source smoothly accelerated through the sound speed. The points  $A$ ,  $B$ ,  $C$ ,  $D$ ,  $E$ ,  $F$  and  $G$  are typical of regions with different wavefield behaviour, as indicated by the different local behaviours of  $Q(\tau)$ .

The expressions (28) and (29) break down as we approach a cusp, which is where  $Q(\tau)$  has an inflection point as in plot  $D$  of Figure 9. Writing

$$\tau = \tau_c + \tau', \quad x = x_c + x', \quad z = z_c + z', \quad (30)$$

where primed variables are small, we see that

$$Q \sim 2(\tau_c^2 - 1)x' - 2(\tau_c^2 - 1)^{3/2}z' - 2\tau_c x' \tau' - \tau_c \tau'^3. \quad (31)$$

Assuming first that we are not too close to the tangent to the cusp  $Z' = 0$ , where

$$Z' = \frac{-x' + (\tau_c^2 - 1)^{1/2}z'}{\tau_c}, \quad (32)$$

we can neglect the penultimate term in (31) to retrieve

$$2^{7/6} \pi \tau_c^{1/2} (\tau_c^2 - 1)^{1/6} \phi \sim \begin{cases} (Z')^{-1/6} \int_1^\infty \frac{dv}{(v^3 - 1)^{1/2}}, & Z' > 0, \\ (-Z')^{-1/6} \int_{-1}^\infty \frac{dv}{(v^3 + 1)^{1/2}}, & Z' < 0. \end{cases} \quad (33)$$

Since

$$\int_{-1}^\infty \frac{dv}{(v^3 + 1)^{1/2}} = 3^{1/2} \int_1^\infty \frac{dv}{(v^3 - 1)^{1/2}} = \frac{1}{2\pi^{1/2}} \Gamma\left(\frac{1}{6}\right) \Gamma\left(\frac{1}{3}\right), \quad (34)$$

the field for  $Z' < 0$  exceeds that for  $Z' > 0$  by a factor of  $3^{1/2}$ . However, if  $Z'$  is sufficiently small, we need to work with the perpendicular coordinate  $X' = ((\tau_c^2 - 1)^{1/2}x' + z')/\tau_c$ . In this situation, the first two terms in (31) can be neglected, leading to the estimate

$$2^{5/4} \pi \tau_c^{1/4} (\tau_c^2 - 1)^{1/8} \phi \sim \begin{cases} (X')^{-1/4} \int_0^\infty \frac{dv}{(v^3 + v)^{1/2}}, & X' > 0, \\ (-X')^{-1/4} \left\{ \int_{-1}^0 + \int_1^\infty \right\} \frac{dv}{(v^3 - v)^{1/2}}, & X' < 0. \end{cases} \quad (35)$$

Here

$$\left\{ \int_{-1}^0 + \int_1^\infty \right\} \frac{dv}{(v^3 - v)^{1/2}} = 2 \int_1^\infty \frac{dv}{(v^3 - v)^{1/2}} \quad (36)$$

$$= 2^{1/2} \int_0^\infty \frac{dv}{(v^3 + v)^{1/2}} = \frac{1}{(2\pi)^{1/2}} \left\{ \Gamma\left(\frac{1}{4}\right) \right\}^2, \quad (37)$$

so that the field for  $X' < 0$  exceeds that for  $X' > 0$  by a factor of  $2^{1/2}$ . We can match (33) and (35) together by considering the region where  $Z' = O(|X'|^{3/2})$ . Here we can write

$$\phi \sim 2^{-5/4} \pi^{-1} \tau_c^{-1/4} (\tau_c^2 - 1)^{-1/8} \rho^{-1/4} I_\pm(\zeta), \quad (38)$$

in  $X' > 0, X' < 0$  respectively, where

$$\rho^2 = X'^2 + Z'^2, \quad \zeta = 2^{-1/2} \tau_c^{3/2} (\tau_c^2 - 1)^{1/4} \rho^{-3/2} Z', \quad (39)$$

and

$$I_{\pm}(\zeta) = \int_{-\infty}^{\infty} \frac{H(v^3 \pm v - \zeta)}{(v^3 \pm v - \zeta)^{1/2}} dv. \quad (40)$$

Equation (38) agrees with (33) and (35) when  $|\zeta| \rightarrow \infty$ , i.e. when

$$\tau_c^{-3/2} (\tau_c^2 - 1)^{-3/4} |X'|^{3/2} \ll |Z'| \ll |X'|. \quad (41)$$

The integral  $I_-$  reveals the discontinuity

$$\Delta I_- = \lim_{\zeta \rightarrow \zeta_1^+} I_-(\zeta) - \lim_{\zeta \rightarrow \zeta_1^-} I_-(\zeta) = -3^{-1/4} \pi \quad (42)$$

at  $\zeta = \zeta_1 = 2/3^{3/2}$ , and the singular term

$$I_{-s} = -3^{-1/4} \ln |\zeta - \zeta_2| \quad (43)$$

at  $\zeta = \zeta_2 = -2/3^{3/2}$ . These agree with (28) and (29) as we move away from the cusp. The similarity variable  $\zeta$  has been anticipated in (10) and the singularities are precisely those identified in §2 for the reflection of a jump discontinuity at a ‘‘Tricomi cusp’’. Indeed, (38) is the solution of (13) subject to (16), (17) and, furthermore, it is in the form (20), but it is in a more convenient form than the Fourier transform discussed after (17). In addition, (38) describes the smooth ‘‘ridge’’ where  $\phi$  is largest on the opposite side  $Z' > 0$  of the cusp, near the positive  $X'$  axis.

Near the source, the jump in  $\phi$  across the Mach envelope is  $\frac{1}{2}(t^2 - 1)^{-1/2}$  to lowest order and the singular part of  $\phi$  on the  $x$ -axis at the back envelope is  $-(2\pi)^{-1}(t^2 - 1)^{-1/2} \ln |x + t - \frac{1}{2} - \frac{1}{2}(t - 1)^{-1} z^2|$ . For  $t < 1$ , when the source is subsonic, the field nearby is

$$\phi \sim -\frac{1}{4\pi} (1 - t^2)^{-1/2} \ln \left( \left( x + \frac{1}{2} t^2 \right)^2 + (1 - t^2) z^2 \right). \quad (44)$$

These results fail near the sonic time  $t = 1$ , which is when this singularity configuration is born, as we now describe.

### 3.3 Birth of the Mach Envelope

Near the sonic time, we replace (30) by

$$t = 1 + t', \quad \tau = 1 + t' + \tau', \quad x = -\frac{1}{2}(1 + t')^2 + x', \quad z = z', \quad (45)$$

where primed variables are again small and  $\tau' \leq 0$ . Then, instead of (31) we have

$$Q \sim -z'^2 - 2x'\tau' - 2t'\tau'^2 - \tau'^3. \quad (46)$$

At the sonic time  $t' = 0$ , (23) can be written asymptotically as

$$\phi \sim (2\pi)^{-1}|z'|^{-1/3} \int_0^\infty \frac{H(v^3 + 2|z'|^{-4/3}x'v - 1)}{(v^3 + 2|z'|^{-4/3}x'v - 1)^{1/2}} dv, \quad z' \neq 0, \quad (47)$$

or

$$\phi \sim 2^{-5/4}\pi^{-1}|x'|^{-1/4} \int_0^\infty \frac{H(v^3 + \text{sgn}(x')v - (2|x'|)^{-3/2}z'^2)}{(v^3 + \text{sgn}(x')v - (2|x'|)^{-3/2}z'^2)^{1/2}} dv, \quad x' \neq 0. \quad (48)$$

These expressions coincide except on the  $x'$  and  $z'$  axes. The field  $\phi$  is of order  $|z'|^{-1/3}$  on  $x' = 0$ , and is of order  $|x'|^{-1/4}$  on  $z' = 0$ .

When  $t' \neq 0$ , the terms in (46) all have equal weight when  $\tau' \sim O(t')$ ,  $x' \sim O(t'^2)$  and  $z' \sim O(|t'|^{3/2})$ . Hence the key to the birth of the Mach envelope is to be found in such a region, the limiting position of the cusps of the previous section being reassuringly found to be at  $\tau' \sim -\frac{2}{3}t'$ ,  $x' \sim \frac{2}{3}t'^2$ ,  $z' \sim \pm (\frac{2}{3}t')^{3/2}$ . We therefore introduce two similarity variables

$$x'_b = \frac{x'}{2t'^2}, \quad z'_b = \frac{2^{-3/2}z'}{|t'|^{3/2}}, \quad (49)$$

so that, with  $\tau' = -2|t'|v$ , (23) becomes

$$\phi \sim 2^{-3/2}\pi^{-1}|t'|^{-1/2} \int_0^\infty \frac{H(v^3 - \text{sgn}(t')v^2 + x'_bv - z'_b{}^2)}{(v^3 - \text{sgn}(t')v^2 + x'_bv - z'_b{}^2)^{1/2}} dv. \quad (50)$$

As  $t'$  increases through zero, (50) describes the strong field near the source just before the birth, as given by (44) for  $t < 1$ , and the result (48) when  $t' = 0$ . Indeed, from (50), (48) also applies when  $t' \neq 0$  as long as  $|x'| \gg t'^2$  or  $|z'| \gg |t'|^{3/2}$ , because the similarity variable  $|x'|/|z'|^{4/3}$  is independent

of  $t'$  from (49). For small positive  $t'$ ,  $\phi$  varies rapidly in an “arrowhead”-shaped region as in the Mach envelope in Figure 2, when shrunk strongly in the  $x$ -direction, and not so strongly in the  $z$ -direction.

#### 4 The Dempsey singularity

While the singularity evolution described above is expected to apply to most of the phenomena associated with two-dimensional sonic boom, Dempsey [2] has proposed a more dramatic singularity resulting from accelerating a source. In the simplest case, the source accelerates from Mach one at a large negative time  $t = t_0$  to infinite Mach number at time  $t = -1$ , so that

$$X(t) = -\sqrt{t^2 - 1}, \quad \text{for } t < -1. \quad (51)$$

The source is switched off at  $t = -1$  so that the right-hand side of (22) is just  $\delta(x - X(t))\delta(z)H(-t - 1)$ . When we consider only the upward-launched boom rays and look at the right-angled triangle  $POF$  in Figure 10, where  $O$  is the origin, perfect focusing will occur at a point  $F$ , as long as the component of the source velocity towards  $F$  equals the sound speed. Hence all boom rays pass through the perfect focus  $F = (0, 1)$ , at

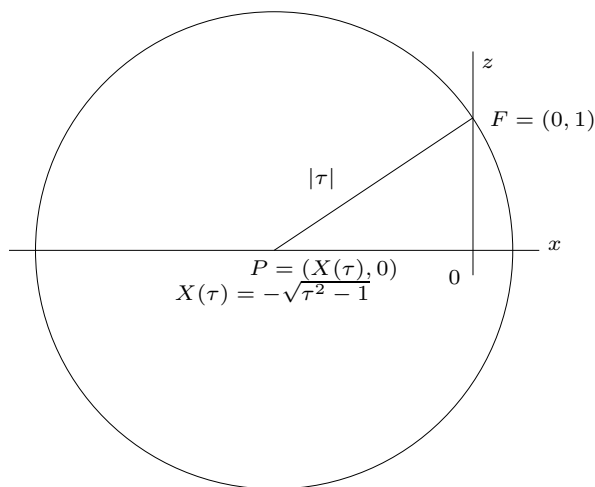


Fig. 10. A perfect focus of boom rays (motion in a straight line).

$t = 0$ . The field  $\phi$  is

$$\phi = \frac{1}{2\pi} \int_{t_0}^t \frac{H(Q(\tau))H(-\tau - 1)d\tau}{\sqrt{Q(\tau)}}, \quad (52)$$

where

$$Q(\tau) = (t - \tau)^2 - (x + (\tau^2 - 1)^{1/2})^2 - z^2 \quad (53)$$

and the Mach envelope is

$$x = -\frac{t}{\tau}(\tau^2 - 1)^{1/2}, \quad z = -\frac{t - \tau}{\tau}, \quad (54)$$

where  $t_0 \leq \tau \leq \min(-1, t)$ . It is always part of the circle

$$x^2 + (z - 1)^2 = t^2, \quad (55)$$

but it takes different forms in the time intervals  $t < -1$ ,  $-1 < t < 0$ , and  $t > 0$ , as shown in Figures 11(a), 11(b), 11(d). In the figures, the solid arc is the Mach envelope, the dashed arc is part of the wavefront  $x^2 + z^2 = (1 + t)^2$  from the origin at  $t = -1$  and the nearly vertical dashed line is the wavefront from  $x = z = 0, t = t_0$ . The perfect focus at  $(0, 1)$  occurs at time  $t = 0$ , when the Mach envelope consists instantaneously of this single point.

(i)  $t < 0$ . On the Mach envelope for  $t < 0$ , the pressure field has a discontinuity because, as in Figure 9, a local maximum of  $Q(\tau)$  passes downwards through zero as the Mach envelope is crossed from “behind” to “ahead”. A local analysis near this maximum shows that the jump from ahead to behind is

$$\Delta\phi = \left\{ \frac{\tau(\tau - 1)(\tau + 1)}{4t} \right\}^{1/2}. \quad (56)$$

Since (54) and (55) give

$$\tau = \frac{t}{1 - z} = -\frac{\{x^2 + (1 - z)^2\}^{1/2}}{1 - z}, \quad (57)$$

we obtain

$$\Delta\phi = -\frac{x}{2(1 - z)^{3/2}}. \quad (58)$$

Thus, in Figure 11(b),  $\Delta\phi \rightarrow \infty$  as  $(x, z)$  approaches the left-most point  $(t, 1)$ , whereas  $\Delta\phi \rightarrow 0$  as  $(x, z)$  approaches the right-most point  $(0, 1 + t)$ . The transition between large and small  $\Delta\phi$  takes place in the region  $1 - z \sim (-x)^{2/3}$ , which is close to the  $z$ -axis. Thus the region of small  $\Delta\phi$  is the vicinity of an upward-pointing cusp at  $(0, 1)$ .

(ii)  $t > 0$ . For  $t > 0$ , the field has a logarithmic singularity on the Mach envelope because a local minimum of  $Q$  passes upwards through zero as the Mach envelope is crossed from right to left. A local analysis near this minimum of  $Q$ , similar to that leading to (29), shows that the singular part  $\phi_s$  of the field on a line of fixed  $z$  is

$$\phi_s = -\frac{1}{\pi} \left\{ \frac{\tau(\tau - 1)(\tau + 1)}{-4t} \right\}^{1/2} \ln |x - x_E|, \quad (59)$$

where  $x_E$  is the value of  $x$  at which the line of fixed  $z$  intersects the Mach envelope, while  $\tau$  is the corresponding emission time. Thus (57) gives

$$\Delta\phi = -\frac{1}{2\pi} \frac{x}{(z - 1)^{3/2}} \ln |x - x_E|. \quad (60)$$

This is the singularity at the solid curve in Figure 11(d). The coefficient in (60) tends to infinity as  $(x, z)$  approaches  $(t, 1)$ , and it tends to zero as  $(x, z)$  approaches  $(0, 1+t)$ . The transition between large and small values of the coefficient now takes place where  $z - 1 \sim x^{2/3}$ , so that the region of small values of the coefficient lies near a downward-pointing cusp at  $(0, 1)$ .

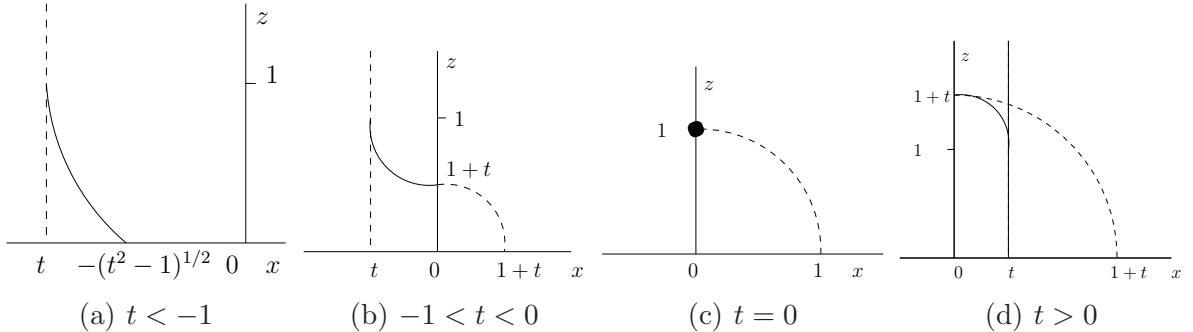


Fig. 11. Mach envelopes for the Dempsey singularity.

As pointed out in [2], [8] perfect focusing can also occur when a point source moves along an equiangular spiral, in which case the Mach envelope consists of a smooth component terminating in a perfect focus. However, all such highly symmetric focusing is structurally unstable because any small perturbation to the sound speed or source path will lead to curvature variations in the Mach envelope, which, in turn, will produce swallowtails in the Mach envelope near a perfect focus.

In all the two-dimensional configurations described so far, we can char-

acterise Mach envelopes and their singularities in terms of travel times along boom rays. If we consider two signals emitted from the source at time  $\Delta t$  apart then, at a smooth Mach envelope, the two signals arrive with a time difference of order  $(\Delta t)^2$ . However at a cusp the two signals arrive with a time difference of order  $(\Delta t)^3$  and  $Q$  needs locally to be approximated by a cubic in  $\tau$ , and, at a perfect focus, there is no time difference at all. In the Appendix we will mention a situation where the two signals arrive with a time difference of order  $(\Delta t)^4$  in connection with the birth of a swallowtail.

## 5 Waves in a three-dimensional homogeneous atmosphere

When (22) is replaced by

$$-\frac{\partial^2 \phi}{\partial x^2} - \frac{\partial^2 \phi}{\partial y^2} - \frac{\partial^2 \phi}{\partial z^2} + \frac{\partial^2 \phi}{\partial t^2} = \delta(x - X(t))\delta(y)\delta(z)H(t), \quad (61)$$

the retarded potential solution analogous to (23) becomes

$$\phi = \frac{1}{4\pi} \int_0^t \frac{\delta(t - \tau - \sqrt{(x - X(\tau))^2 + y^2 + z^2})}{\sqrt{(x - X(\tau))^2 + y^2 + z^2}} d\tau. \quad (62)$$

This gives (Bateman [4], p.115; Guiraud [5], p. 218)

$$\phi = \frac{1}{2\pi} \sum_{Q(\tau)=0} \left| \frac{\partial Q}{\partial \tau} \right|^{-1}, \quad (63)$$

where now  $Q(\tau) = (t - \tau)^2 - (x - X(\tau))^2 - y^2 - z^2$  and the sum is taken over those values of  $\tau$  for which  $Q(\tau) = 0$  and  $\tau \leq t$ . In contrast with §3, we now only have the algebraic task of solving  $Q(\tau) = 0$  and computing  $\partial Q/\partial \tau$ . Also, by symmetry, we need only consider the solution in the  $(x, z)$  plane.

### 5.1 Impulsive motion

When the source is in steady supersonic motion after starting impulsively, the wavefronts and Mach envelope are generated by revolving the wavefronts and the Mach wedge in Figure 1 about the  $x$ -axis. However, the

wavefield now has an inverse square root singularity as we approach the Mach envelope, which is now the familiar Mach cone, from the interior. This is in accordance with the fundamental solution of (1) in the aerodynamic frame. Moreover, the sum of the contributions from the two zeros of  $\partial Q/\partial\tau$  which emerge as we cross the Mach envelope from the outside is non-constant. Hence, in accordance with Huygens' principle, the wavefield is always non zero inside the Mach envelope and it remains of  $O(1)$  at distances of  $O(1)$  from the source for all time.

For an accelerating source, the Mach envelope is given by rotating (25) about the  $x$ -axis. On the incident part of the Mach envelope and away from the cusp, with  $t^{1/3} < \tau < t$ , the passage of a local maximum of  $Q$  through zero shows that  $\phi$  jumps from zero to

$$\phi = 2^{-3/2}\pi^{-1}\tau(t-\tau)^{-1/2}(\tau^3-t)^{-1/2}(x-x_E)^{-1/2}, \quad (64)$$

instead of (28);  $x_E$  is the value of  $x$  at which a line  $z = \text{constant}$  meets the Mach envelope [8]. Equation (64) can be written as

$$\phi = 2^{-7/4}3^{-1/4}\pi^{-1}(t-\tau_c)^{-1/2}(x_c-x)^{-1} \left( \frac{x-x_E}{(x_c-x)^{3/2}} \right)^{-1/2}, \quad (65)$$

as the cusp is approached, the final term suggesting the similarity variable to be used near the cusp. In contrast to the two-dimensional case, on the back envelope where  $1 \leq \tau < t^{1/3}$ , the three-dimensional calculation is very similar to that for near the incident part of the Mach envelope; there is no asymmetry as there was between (28) and (29). The singular part of  $\phi$  is

$$\begin{aligned} \phi_s &= 2^{-3/2}\pi^{-1}\tau(t-\tau)^{-1/2}(t-\tau^3)^{-1/2}(x_E-x)^{-1/2} \\ &\sim 2^{-7/4}3^{-1/4}\pi^{-1}(t-\tau_c)^{-1/2}(x_c-x)^{-1/4}(x_E-x)^{-1/2}, \end{aligned} \quad (66)$$

as  $\tau \rightarrow \tau_c$ , where  $x_E$  is now the value of  $x$  at the back envelope on a line  $z = \text{constant}$ .

In the neighbourhood of the cusp we again have different representations on the two sides of the tangent to the cusp, i.e. in  $Z' > 0$ ,  $Z' < 0$ , where

$Z'$  is defined in (32). The results, which are analogous to (33), are

$$\phi \sim \begin{cases} 2^{-5/3} 3^{-1} \pi^{-1} \tau^{-1} (\tau^2 - 1)^{-2/3} (-Z')^{-2/3}, & Z' < 0, \\ 2^{-5/3} 3^{-1} \pi^{-1} \tau^{-1} (\tau^2 - 1)^{-2/3} (Z')^{-2/3}, & Z' > 0. \end{cases} \quad (67)$$

Here the coefficient for  $Z' < 0$  is the same as that for  $Z' > 0$ , in contrast to (33). For small  $Z'$ , the results analogous to (35) are

$$\phi \sim \begin{cases} \frac{1}{4\pi} (\tau^2 - 1)^{-1/2} (X')^{-1}, & X' > 0, \\ \frac{1}{2\pi} (\tau^2 - 1)^{-1/2} (-X')^{-1}, & X' < 0, \end{cases} \quad (68)$$

so that the field jumps by a factor of 2 across  $X' = 0$ . Finally, in the matching region where  $Z' = O(|X'|^{3/2})$ , the result analogous to (40), (42) is, in  $X' > 0$ ,

$$\phi \sim \frac{1}{4\pi} (\tau^2 - 1)^{-1/2} \rho^{-1} |3v^2(\zeta) + 1|^{-1}, \quad (69)$$

where

$$\zeta = 2^{-1/2} \tau^{3/2} (\tau^2 - 1)^{1/4} \rho^{-3/2} Z', \quad (70)$$

and  $v(\zeta)$  is the unique real root of  $v^3 + v - \zeta = 0$ . Meanwhile, in  $X' < 0$ , there are three contributions from the three real roots  $v_i$  of  $v^3 - v - \zeta = 0$ , where  $\zeta$  is still given by (70), and hence

$$\phi \sim \frac{1}{4\pi} (\tau^2 - 1)^{-1/2} \rho^{-1} \sum_{i=1}^3 |3v_i^2(\zeta) - 1|^{-1}. \quad (71)$$

As in the two-dimensional case, it is easy to verify that these results match with (67)–(68) as  $\zeta \rightarrow \infty$ . The singularities analogous to (43) are

$$\phi \sim \begin{cases} 3^{-1/4} (4\pi)^{-1} (\tau^2 - 1)^{-1/2} \rho^{-1} (2/3^{3/2} - \zeta)^{-1/2} & \text{when } \zeta < 2/3^{3/2}, \\ 3^{-1/4} (4\pi)^{-1} (\tau^2 - 1)^{-1/2} \rho^{-1} (\zeta + 2/3^{3/2})^{-1/2} & \text{when } \zeta > -2/3^{3/2}. \end{cases} \quad (72)$$

Here the coefficient for  $\zeta < 2/3^{3/2}$  is the same as that for  $\zeta > -2/3^{3/2}$ . Since the wavefield near the cusp is locally two-dimensional, there must still be a region near the cusp where the solution satisfies a Tricomi equation of the form (10). Indeed, in the same way that (38) satisfied such a Tricomi equation, so does (69). Whereas the former described the conversion of an incoming jump singularity to an outgoing logarithmic one, (69) describes the conversion of an incoming inverse square-root

singularity to an outgoing one. Also (69) is of the form (20), with  $F$  being a delta function.

For  $t < 1$ , when the source is subsonic, the local field is such that

$$\phi \sim \frac{1}{4\pi} \left( \left( x + \frac{1}{2}t^2 \right)^2 + (1 - t^2)z^2 \right)^{-1/2}, \quad (73)$$

in contrast to (44).

### 5.2 Birth of the Mach Envelope

Near the sonic time, we again use (45), but (46) must be replaced by

$$Q \sim -z'^2 - x'^2 - 2x'\tau' - 2t'\tau'^2 - \tau'^3. \quad (74)$$

At the sonic time  $t' = 0$ , (63) gives the approximate functional forms

$$\phi \sim |z'|^{-4/3} f(|z'|^{-4/3}x'), \quad (z' \neq 0) \quad (75)$$

and

$$\phi \sim |x'|^{-1} g(|x'|^{-3/4}z', \text{sgn}(x')), \quad (x' \neq 0) \quad (76)$$

(cf. (48)) where the functions  $f$  and  $g$  are obtained by solving the cubic equation  $Q(\tau') = 0$ , with  $Q$  given by (74). In particular, when  $|x'| \ll |z'|^{4/3}$ , (75) gives  $\phi \sim \frac{1}{6}\pi^{-1}|z'|^{-4/3}$ , and when  $|x'| \gg |z'|^{4/3}$ , (76) gives  $\phi \sim \frac{1}{4}\pi^{-1}x'^{-1}$  for  $x' > 0$ , and  $\phi \sim \frac{1}{8}\pi^{-1}(-x')^{-1}$  for  $x' < 0$ . These results depend on the fact that for  $t' = 0$  the three roots  $\tau'$  of  $Q(\tau') = 0$  all scale as  $|z'|^{2/3}$  for  $|x'| \ll |z'|^{4/3}$  or  $|x'| \sim |z'|^{4/3}$ , but scale separately as  $|x'|^{1/2}$ ,  $|x'|^{1/2}$  and  $(x'^2 + z'^2)/|x'|$  for  $|x'| \gg |z'|^{4/3}$ .

For  $t' > 0$ , an arrowhead envelope is again present, governed by the same equations as for the two-dimensional problem. The cusps occur for  $\tau' \sim -\frac{2}{3}t'$  and are at  $x' \sim \frac{2}{3}t'^2$ ,  $z' \sim \pm(\frac{2}{3}t')^{3/2}$ . A scaling analysis analogous to that of (49), (50) shows that for  $t' \neq 0$  the field contains an inner region in the form of a box defined by  $|x'| \leq O(t'^2)$ ,  $z' \leq O(|t'|^{3/2})$  within which the field has the approximate form

$$\phi \sim |t'|^{-2} h(|t'|^{-2}x', |t'|^{-3/2}z', \text{sgn}(t')), \quad (77)$$

where the function  $h$  is obtained from the roots of the cubic equation  $Q(\tau') = 0$ . This inner region exists not only for  $t' > 0$ , when it contains

the arrowhead and its cusps, but also for  $t' < 0$ , when it is a region of high pressure which exists just before the birth of the arrowhead. This high pressure region presages the birth of the arrowhead. In (77) the form of  $h$  is such that the limit  $|x'| \gg |t'|^2$  or  $|z'| \gg |t'|^{3/2}$ , or both, recovers (76) or (75). Thus the results we derived above for  $t' = 0$  also apply for  $t' \neq 0$  outside the inner region.

### 5.3 Other singularities in three dimensions

The discussions in §3.2 and §5 have revealed that the focusing that occurs at a cusp in the Mach envelope is locally described by a Tricomi equation, no matter whether the flow is two-dimensional or axisymmetric. However, the singularities that occur in the far field of the solution of the Tricomi equation are quite different in two and three dimensions; for a *line source* in a two-dimensional flow these singularities are of the “jump-log” type but for a *point source* in a three-dimensional flow there is a switch from one inverse square root to another<sup>6</sup>. Corresponding similarities and contrasts occur in other situations and we will give just two examples.

(i) Point sources moving supersonically. It is easy to write down the wavefronts and boom rays and hence plot a Mach envelope typified by Figure 12. However we cannot reduce the three-dimensional version of (13) to (14) without either performing a Fourier analysis or repeating the asymptotics leading to (10). Nonetheless, as in any axisymmetric problem driven by a point source on the axis, there will be a “square root” to “square root” switch between the two branches of the Mach envelope at any point of the cusp locus in Figure 12.

(ii) The Dempsey singularity in three dimensions. In three dimensions the effect of the source motion (51) is to produce a perfect focus at  $t = 0$  in the plane  $x = 0$  on the circle  $r^2 = y^2 + z^2 = 1$ . The diagrams of the wavefronts and Mach envelope are obtained by rotating those for two dimensions about the  $x$ -axis. For  $t < 0$ , as distinct from the “jump-log”

---

<sup>6</sup> These different configurations could be reconciled by considering a distribution of three-dimensional point sources along the  $y$ -axis in a non-axisymmetric flow. Near the middle of this distribution, cusps in the Mach envelope would have approximately jump-log singularities and near the ends they would have square root-square root singularities.

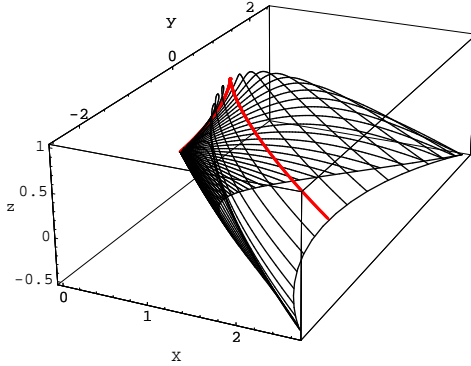


Fig. 12. Bicharacteristics for the model atmosphere  $c = 2/(2 - z)$  with source speed  $U = \sqrt{2}$ . They are truncated at  $z = z_g = -1/2$  and the corresponding carpet is plotted. The bicharacteristic in the  $x$ - $y$  plane through the source is plotted with a thicker line—it has its maximum at the sonic line  $z = 1$ . This maximum is a cusp, as in the two-dimensional geometry of Figure 5.

singularity which would arise from a line source, there is an inverse square root singularity on the quarter-circular arc  $x^2 + (1 - r)^2 = t^2$ ,  $x < 0$ ,  $r < 1$ , with the local form

$$\phi_s \sim -\frac{x}{2\pi(1-r)\sqrt{r}} \frac{1}{\sqrt{(1-r)^2 + x^2 - t^2}}, \quad (78)$$

analogous to the discontinuity (58) in the two-dimensional case. When  $t > 0$ , this is converted into an outgoing inverse square root singularity in the region  $x > 0$ ,  $r > 1$ , having the same form.

## 6 Discussion and Conclusion

The main aim of this paper has been to elucidate the details of the acoustic field in the vicinity of the singularities that are most likely to occur when a wave field is generated by a supersonic source. The generic singularity is that at a smooth component of the Mach envelope. Near the source the singularity is simply that associated with the Mach wedge or Mach cone from the source, but the Mach envelope can easily develop singularities at which more intense acoustic focusing can take place. The generic focusing of the Mach envelope into a cusp, be it produced by inhomogeneities in the atmosphere or accelerations of the source, is always described locally by a Tricomi equation of the form (11). However, as described in §3.3, there is a complicated sectoral structure to the wave-field near the cusp and the solution of the full wave equation is needed to

delineate this structure. The Tricomi equation describes the most intense amplitudes and it captures the transition in the singularities that occur at the Mach envelope components on either side of the cusp.

We have derived, in §4, the extreme (but non-generic) focusing of the wavefield that was suggested by Dempsey [2], in which a violent singularity occurs at one point of space and one instant of time. Between these singularities and the Mach envelope cusp, other kinds of intermediate focusing can occur. For example, the Mach envelope can develop a new locus of cusp singularities through a swallowtail. This is illustrated in the Appendix, and is also generic. Alternatively, a source could accelerate continuously from rest into a Dempsey-like focusing motion, *e.g.*

$$X(t) = \begin{cases} -t^2/2 & \text{for } t \leq M_0; \\ -(3M_0^2/2 - 1 - \sqrt{(M_0^3 - t)^2 - (M_0^2 - 1)^3}) & \text{for } M_0 \leq t \leq M_0^3 - (M_0^2 - 1)^{3/2}. \end{cases} \quad (79)$$

An example of this for  $M_0 = 2$  is shown in Figure 13.

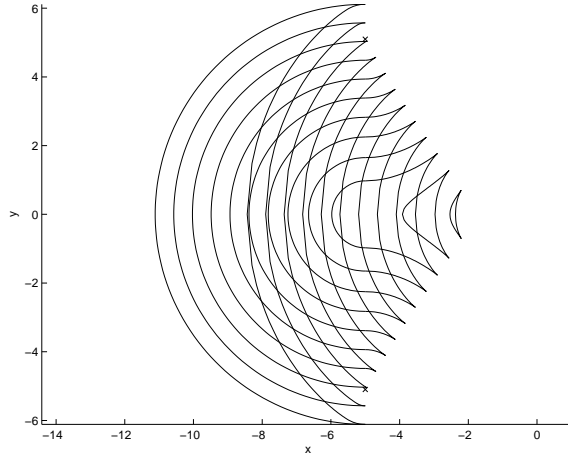


Fig. 13. Trace of the Mach cone on the ground ( $z = -1$ ) for a source moving as in (79) with  $M_0 = 2$ . The form of the envelope due to constant acceleration (on the right) develops inwardly focusing arcs with foci at the points marked  $\times$  where the Dempsey focal circle intersects the ground.

Although it was not our primary aim to give a detailed account of the implications of our singularity analysis for the sonic boom heard at ground level beneath a supersonic source, we will conclude with three observations concerning the “carpet” of the wavefield.

- (i) For the primary boom of a smoothly accelerating source, the carpet created by the Mach envelope and the cusp locus are contrasted with the carpet caused by an impulsive source in Figures 14(a) and 14(b).

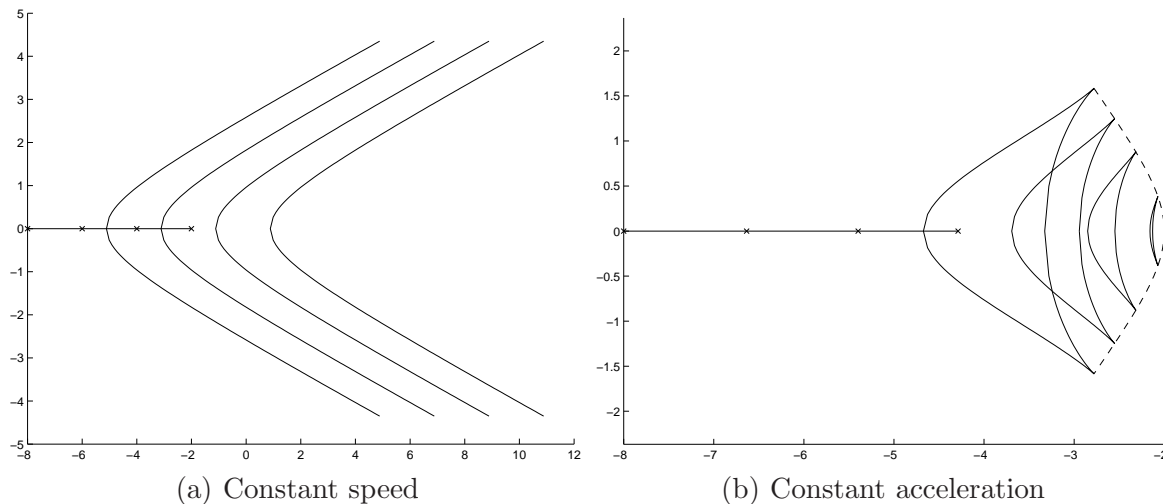


Fig. 14. The trace of the Mach cone on the ground ( $z = -1$ ) for an aircraft moving to the left in a uniform atmosphere. The position of the sonic boom on the ground is plotted for the times when the aircraft is at the 4 marked positions. In (a) the speed is constant,  $X(t) = -2t$ . In (b) the acceleration is constant,  $X(t) = -t^2/2$ .

- (ii) In a homogeneous atmosphere, it is possible to contrive acceleration profiles which produce more intense focusing at certain times and positions than does the cusp locus of Figure 14(b), while being less intense than the Dempsey singularity. These profiles can be characterised by the arrival time differences mentioned at the end of § 4. When these are of order  $(\Delta t)^4$  a typical carpet for  $y > 0$  is shown in Figure 15.
- (iii) For the secondary boom generated by steady motion in the atmosphere  $c^2 = 2/(2 - z)$  in which there is a sonic height, the Mach envelope (spanned by bicharacteristics) is illustrated in Figure 12 and the corresponding carpet in Figure 16. The reflection of sonic boom from the ground and subsequent refraction in the atmosphere has not been included here, but will of course add further features to the ground carpet.

### Acknowledgements

We thank M. Taroni for his assistance with the calculations relating to the accelerating source while he was in receipt of an undergraduate summer bursary at the University of Keele. Also, K. Kaouri acknowledges the support of the Sonic Boom European Research Programme (SOBER, G4RD-CT-2000-00398).

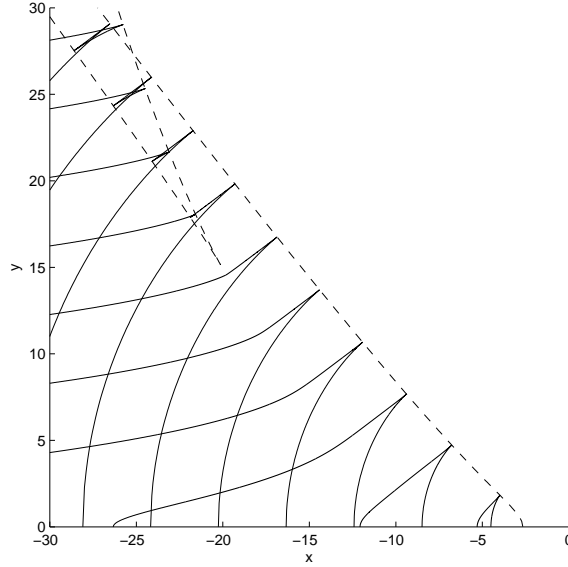


Fig. 15. Trace of the Mach envelope on the ground  $z = -1$  in the region  $y > 0$ , for a source accelerating from rest with  $\ddot{X}(t) = -(1 - t/5)^2$ . Two new cusps are formed on the Mach envelope via a swallowtail, where the arrival time differences are  $O(\Delta t)^4$ . The locus of the cusps on the ground is the dashed line.

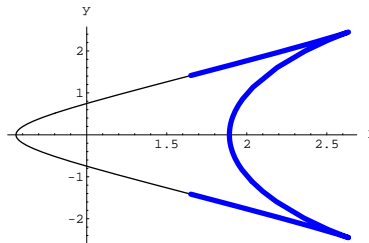


Fig. 16. The carpet for  $B^2 = 1 - z$  at  $z = z_g = -1/2$ . The primary and secondary carpets are joined because all bicharacteristics that are launched upwards reflect at a certain height (according to generalised Snell's law) and eventually reach  $z_g$ .

## References

- [1] F.G. Friedlander, Sound Pulses, Cambridge University Press, 1958.
- [2] D.F. Dempsey, Focusing conditions for sonic booms. J. Acoust. Soc. Amer., 61(3):655–658, 1977.
- [3] L. Howarth, The propagation of steady disturbances in a supersonic stream bounded on one side by a parallel subsonic stream. Proc. Cam. Phil. Soc. 44:380–390, 1948.
- [4] H. Bateman, The Mathematical Analysis of Electrical and Optical Wave-Motion on the basis of Maxwell's Equations, Dover, 1955.
- [5] J-P. Guiraud, Acoustique géométrique, bruit balistique des avions supersoniques et focalisation. J. Méc., 4:215–267, 1965.
- [6] M.J. Lighthill, Reflection at a laminar boundary layer of a weak steady disturbance to a supersonic stream, neglecting viscosity and heat conduction. Q. J. Mech. Appl. Math. 3:303–325, 1950.

- [7] G.M. Lilley, R. Westley, A.H. Yates, and J.R. Busing, Some aspects of noise from supersonic aircraft. *J. Roy. Aero. Soc.* 57:396–414, 1953.
- [8] K. Kaouri, Secondary Sonic Boom. DPhil thesis, University of Oxford, 2004. (<http://eprints.maths.ox.ac.uk/view/type/thesis.html>)
- [9] R.P. Rosales and E.G. Tabak, Caustics of weak shock waves. *Phys. Fluids*, 10(1):206–222, 1998.
- [10] W.J. Strang, A physical theory of supersonic aerofoils in unsteady flow. *Proc. Roy. Soc. Lond. A* 195:245–264, 1948.
- [11] W.J. Strang, Transient source, doublet and vortex solutions of the linearized equations of supersonic flow. *Proc. Roy. Soc. Lond. A* 202:40–53. 1950.
- [12] W.J. Strang, Transient lift of three-dimensional purely supersonic wings. *Proc. Roy. Soc. Lond. A* 202:54–80, 1950.
- [13] B. Sturtevant and V.A. Kulkarny, The focusing of weak shock waves. *J. Fluid Mech.*, 73:651–671, 1976.

## A Two-dimensional accelerating motion in a stratified atmosphere

For a constant acceleration source at  $(-\frac{1}{2}t^2, 0)$  in a stratified medium with sound speed profile  $c = 1/\sqrt{1-z}$ , it is shown in [8] that there are singularities of higher order than those discussed in §2 and §3. The motion is supersonic when  $t \geq 1$  and the boom rays at  $t = 3$  are plotted in Figure A.1.<sup>7</sup>

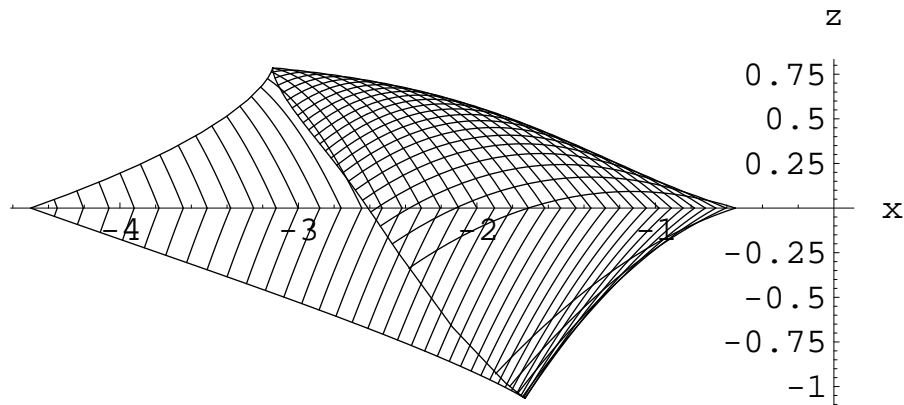


Fig. A.1. Constant acceleration in the stratified medium with sound speed profile  $c = 1/\sqrt{1-z}$ . The boomrays are illustrated for  $t = 3$ ,  $\tau = 1.01$  to  $\tau = 2.9$  (in increments of 0.01). The Mach envelope is also plotted and has 2 cusps.

In Figure 5 only upward-launched boomrays form an envelope but in Figure A.1 and Figure 3 both upward and downward launched boomrays form envelopes. These envelopes of boomrays are also loci of the cusps on the Mach envelope. The upper cusp locus starts at  $z = 0$  and goes

<sup>7</sup> The Mach envelope is still determined analytically.

up to  $z \approx 0.75$ , and the lower starts at  $z = 0$  and goes down to  $z \approx -1$ . The Mach envelope is open in Figure 5 and closed in Figure 3 and Figure A.1, consisting of an incident (“Mach wedge”-like) and a reflected component.

As  $t$  increases further, we see in Figure A.2 that the reflected envelope component changes curvature (at about  $t = 5$ ), and at about  $t = 8$  it develops a curvature discontinuity. This discontinuity corresponds to a travel time delay of order  $(\Delta t)^4$  in the discussion at the end of §4.

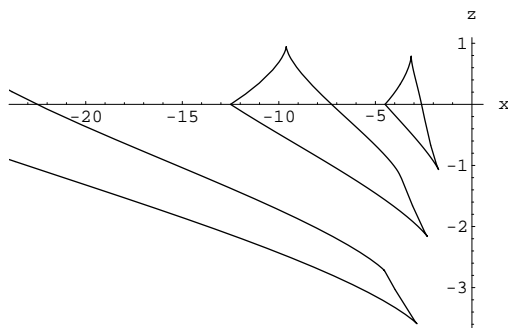


Fig. A.2. The Mach envelope for  $t = 3$ ,  $t = 5$ ,  $t = 8$ . It is a closed curve (for all times) and the part formed by upward-launched boom rays has an incident and a reflected component. By the time  $t = 5$  the curvature of the reflected component has changed. A ‘kink’ develops for  $t \approx 8$ , giving rise to two cusps. (The envelope for  $t = 8$  is very elongated in the  $x$ -direction so not all of it is shown.)

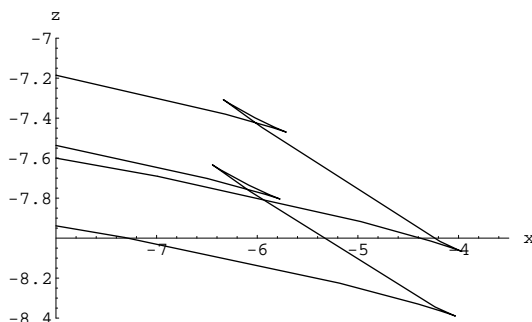


Fig. A.3. The Mach envelope for  $t = 20$  and  $t = 21$ : magnified view of the new cusps near  $x = -6$  which are produced by the formation of a cusp caustic of boom rays. The lower original cusp is also shown on each envelope.

As  $t$  increases further, the Mach envelope forms a swallowtail and so gives rise to two *new* cusps. Such swallowtails correspond to the formation of a so-called *cusp caustic* of boom rays: they have been observed experimentally by Sturtevant and Kulkarny [13], and our example shows that they can arise in a sonic boom scenario. In Figure A.3 we show a magnified version of these new cusps at times  $t = 20$  and  $t = 21$ .